

High-frequency transverse oscillations and intensity perturbations in spicular-type events

J. Shetye¹, D. Kuridze², M. Stangalini³, J. G. Doyle¹, E. Scullion⁴, V. Henriques², T. Ray⁵

¹Armagh Observatory and Planetarium, College Hill, Armagh BT61 9DG, N. Ireland

²Astrophysics Research Centre, School of Mathematics and Physics, Queen's University Belfast, BT7 1NN, N. Ireland

³INAF-OAR National Institute for Astrophysics, 00040, Monte Porzio Catone (RM), Italy

⁴Department of Mathematics Physics and Electrical Engineering, Northumbria University, Newcastle upon Tyne, UK

⁵Dublin Institute for Advanced Studies, 31 Fitzwilliam Place, Dublin 2, Ireland

Received date, accepted date

ABSTRACT

Context. It is widely accepted that chromospheric fine structures are waveguides for several types of magnetohydrodynamic (MHD) oscillations, which can transport energy from the lower to upper layers of the Sun. Despite a number of recent advances in the field, a detailed study of the properties and physical nature of these oscillations remains a challenging task.

Aims. Here we aim to study high-frequency transverse oscillations and intensity variations of spicular-type H α features in an active region.

Methods. We investigated high-resolution spectroscopic and imaging observations from the CRisp Imaging SpectroPolarimeter (CRISP) instrument on the Swedish 1-meter Solar Telescope (SST) to study the dynamics of chromospheric spicular structures. Time-distance analyses were used to examine the characteristics of the transverse (incompressible) and intensity (compressible) perturbations. The relationship between these incompressible and compressible oscillations were also investigated through direct comparisons of the fluctuations.

Results. We detect transverse oscillations in chromospheric spicules at different positions along their length in both the vertical and horizontal directions with respect to the image plane. We also find a link between intensity perturbations and the horizontal velocity fluctuations of the flux tube.

Conclusions. The observed oscillations are interpreted in terms of MHD helical kink waves. The link between intensity and horizontal velocity oscillations can be explained by the coupling of compressive with non-compressive waves and by the interaction of the flux tube with its neighbours. This leads to compressive perturbations correlated to the horizontal displacement of the tube itself.

Key words. Sun: chromosphere - Line: profiles - Methods: observational

1. Introduction

Solar spicules are dynamic, jet-like structures lasting up to a few minutes in the solar atmosphere that are mainly observed in the chromosphere (Beckers 1968, 1972; Tsiropoula et al. 2012, and references therein). When observed on the limb, these are classified as Type I or Type II spicules (De Pontieu et al. 2007b; Pereira et al. 2012), and on disk they are identified as Rapid Blue/Red-Shifted Excursions (termed as RBE or RREs, Langangen et al. 2008; Rouppe van der Voort et al. 2009; Sekse et al. 2013a,b; Kuridze et al. 2015; Henriques et al. 2016; Kuridze et al. 2016, and references therein). Recently, both ground- and space-based observations have shown different types of waves and oscillations in these structures. Such oscillations are identified through the study of intensity, Doppler, and displacement perturbations (Kukhianidze et al. 2006; Zaqarashvili et al. 2007; De Pontieu et al. 2007a; He et al. 2009a,b; Zaqarashvili & Erdélyi 2009; Okamoto & De Pontieu 2011; Kuridze et al. 2012, 2013; Morton et al. 2012; Shetye et al. 2016a; Pereira et al. 2016). The most prominent wave signatures detected in these chromospheric fine structures are the transverse oscillations of their longitudinal axis, which can be interpreted as fast kink magnetohydrody-

namic(MHD) waves (see review by Zaqarashvili & Erdélyi 2009).

The transverse displacement in spicules was initially noted by Nikolsky & Platova (1971) within solar limb observations. The authors showed that some spicules change their position along the slit, thereby showing a horizontal component of velocity. They concluded that spicules can support quasi-periodic oscillations parallel to the limb with a period of ~ 1 min, a displacement amplitude of 725 km, and velocity amplitudes around $10 - 15 \text{ km s}^{-1}$. Later, Kukhianidze et al. (2006) studied spicules at eight different heights ranging from 3800 to 8700 km. They found that $\sim 20\%$ of the data series showed an oscillatory behaviour in the Doppler velocities, orthogonal to the structures, with a wavelength of 3500 km and periods in the range of 35 – 70 s, suggesting the presence of transverse kink waves. Observations with the Solar Optical Telescope onboard Hinode have identified ubiquitous transverse motion in spicules (De Pontieu et al. 2007c).

Kuridze et al. (2012, 2013) detected propagating and standing MHD kink waves in H α core mottles, which are considered as the disk counterparts of Type I limb spicules. Evidence of periodic transverse motions in relatively short-lived RBEs has been reported by Sekse et al. (2013b). Transverse motions are not the only wave motions observed in chromospheric spicular jets.

Morton et al. (2012) detected an out-of-phase behaviour of periodic perturbations in intensity and width and interpreted this as compressible sausage wave modes in chromospheric flux tubes. Furthermore, recent observations show that RBEs or RREs and Type II spicules undergo torsional or twisting motions during their evolution (De Pontieu et al. 2012, 2014).

Ubiquitous MHD waves observed in chromospheric fine structures are thought to play a major role in transferring energy from the lower solar atmosphere into the chromosphere and corona, where they can dissipate as heat (Cranmer et al. 2007). Despite many theoretical efforts, the dissipation mechanism of the waves with low-frequency has not yet been well understood. However, higher frequency waves are more readily dissipated through ion-neutral damping if the wave frequency becomes close to the gyro-frequency of the ions in the plasma. Detecting high-frequency waves in the chromospheric spicules is extremely challenging because of the limitations in the spatial and temporal resolution of the current instruments; previous efforts include those by Kukhianidze et al. (2006); Zaqarashvili et al. (2007), and He et al. (2009a). It must be noted that chromospheric jets are considered to be travelling along magnetic flux tubes, which can guide different types of MHD waves. The alignment of chromospheric structures with the magnetic field was investigated by de la Cruz Rodríguez & Socas-Navarro (2011) who compared the orientation of chromospheric fibrillar structures to that of the sunspot magnetic field obtained via high-resolution spectro-polarimetric observations of Ca II lines. Most of the fibrillar structures traced well the chromospheric magnetic field, although exceptions were noted. Recently, Leenaarts et al. (2015) also investigated the relation between fibrils/chromospheric fine-scale structures and the magnetic field lines using synthetic $H\alpha$ images computed from a three-dimensional (3D) radiation-MHD simulation of a network region. They found that some fibrils trace out the same field lines along the fibril length, while other fibrils sample different field lines at many locations along their length. Hence, they could not always be used to trace the magnetic field.

This paper follows on from previous work by Shetye et al. (2016b, henceforth Paper1), which investigated the dynamics and statistical properties of spicular-type events. In Paper1 they briefly reported on various transverse motions observed in such events where the computed amplitudes of transverse motions were around 230 km with a period of 20 s and velocities between $15 - 30 \text{ km s}^{-1}$. In this paper, we present a detailed analysis of two selected case-studies that not only show transverse motion, but also suggest mode-coupling. The choice of these two events originates from the fact that the transverse motion is tracked for a longer time than in the other cases as discussed in Appendix A. We provide context images and time-distance diagrams taken at the central positions of the structures presented in Paper1. We bring forth an evidence for possible helical kink waves in these events. Furthermore, we study non-compressive intensity perturbations by investigating a relation between intensity perturbations and the horizontal velocity fluctuations.

In Section 2 we briefly describe the observations and data reduction. The methods used to study the events are described alongside a discussion of the results pertinent to the two cases in Section 3. We discuss the physics of observed perturbations in Section 4. The main findings of the paper are summarised in Section 5.

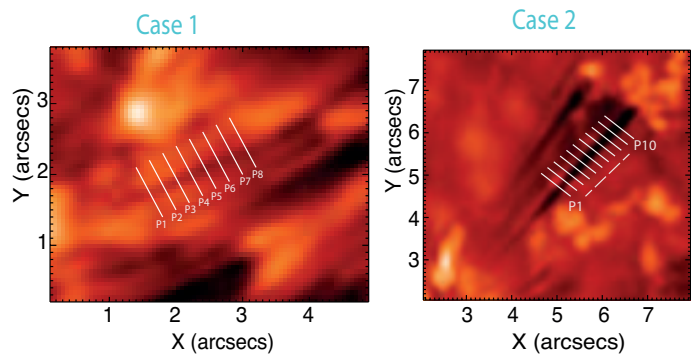


Fig. 1. SST images at $+516 \text{ mÅ}$ from the $H\alpha$ line core showing the two spicules selected for the analyses. The left image is discussed as Case 1 and the image on the right is referred to as Case 2. The white lines indicate the locations chosen for the analysis of the transverse displacement of the structures. For Case 1, we analysed 21 locations along the length of the spicule between P1 and P8 in the image, for Case 2 we analysed 31 locations along the length of the spicule, but present 10 slits between P1 and P10 for clarity.

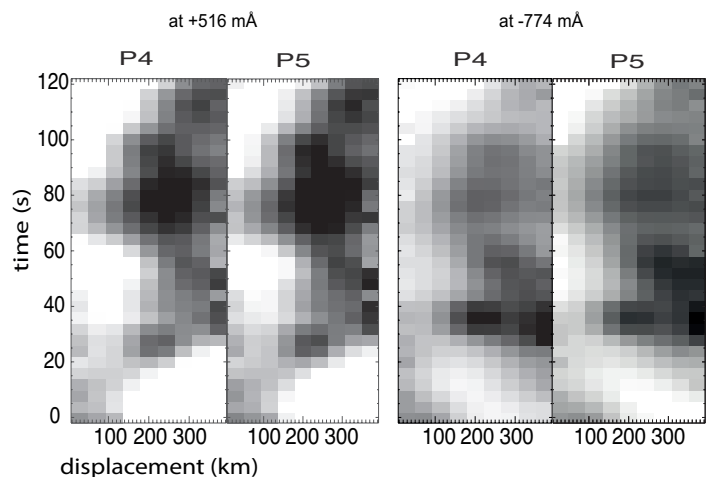


Fig. 2. Time-distance diagrams generated in the -774 mÅ and $+516 \text{ mÅ}$ wavelength positions related to the $H\alpha$ line core at locations (P4, P5), indicated by the white lines in the left panel of Fig. 1 (Case 1).

2. Observations

We used spectral imaging observations taken with the CRISP Imaging SpectroPolarimeter (CRISP, Scharmer et al. 2008) instrument on the Swedish 1 m Solar Telescope (SST, Scharmer et al. 2003). CRISP has a field of view (FOV) of $60'' \times 60''$ with an approximate pixel scale of $0.0592''$. The observations were collected during a 50-minute interval between 07:17 UT and 08:08 UT on 10 June 2014. The FOV of these data was centred at $x_c = 403''$ and $y_c = -211''$, which contained a pore NOAA AR 12080. Nine $H\alpha$ spectral line positions were sampled in sequence, with eight images being collected at each line position, corresponding to $-1032, -774, -516, -258, 0, +258, +516, +774$ and $+1032 \text{ mÅ}$ relative to the line core at 6562.8 Å . After Multi-Object Multi-Frame Blind Deconvolution (MOMFBD, van Noort et al. 2005) reconstruction and the CRISPRED (de la Cruz Rodríguez et al. 2015) pipeline, an effective science-ready cadence of 3.9 s was achieved, meaning these observations are perfect for analysing rapid dynamics in the chromosphere. After co-alignment with SDO/AIA 1700 Å

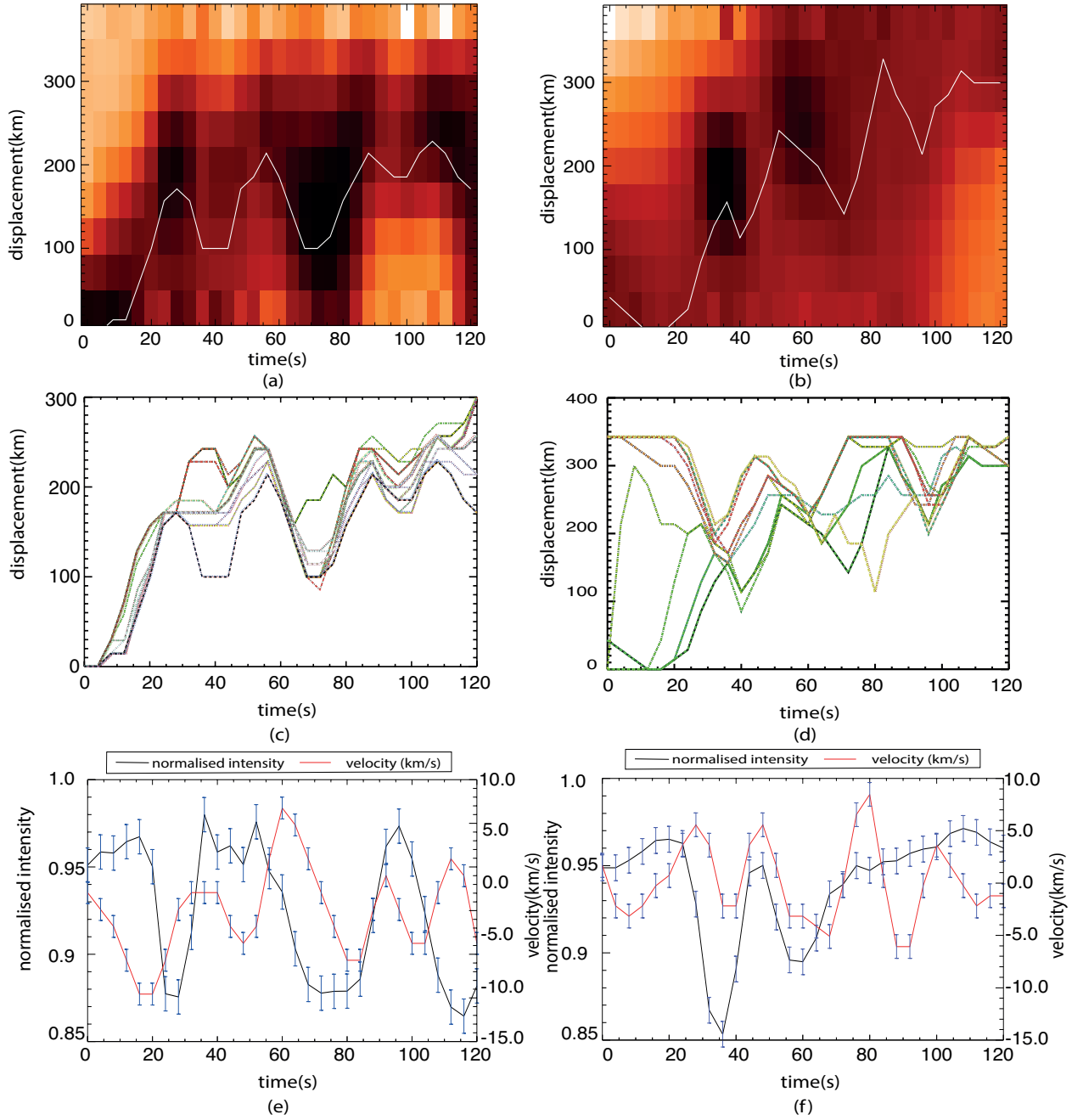


Fig. 3. Top panels: Time-distance diagrams generated from wavelength positions $+516 \text{ mÅ}$ (a) and -774 mÅ (b) at location P8 for the first spicule (Case 1) with the minima corresponding to each time-step shown using a white line. The middle panels (c for $+516 \text{ mÅ}$) and (d for -774 mÅ) show displacement time series at 21 different positions along the length of the structures (in between positions P1–P8). The bottom panels (e for $+516 \text{ mÅ}$) and (f for -774 mÅ) show intensity vs time and velocity vs time. The red and the black solid lines are the velocity and intensity profiles, respectively. The errors bars represent one standard deviation.

images, we determined that the CRISP FOV is tilted at an angle of $+62^\circ$ with respect to the SDO heliocentric FOV. The diffraction limited resolution at $H\alpha$ is $0.14''$. The $H\alpha$ pre-filter FWHM is 4.9 Å while the FWHM of the transmission filter is 60.4 mÅ allowing observations at multiple positions within the $H\alpha$ line profile. The details of the calibration techniques are explained in Paper1.

3. Analyses and results

Figure 1 shows a snapshot of the two spicules investigated in this work. The two images are acquired at $+516 \text{ mÅ}$ from the line core. The white lines drawn perpendicular to the structure indicate some of the locations chosen to analyse transverse displacements and intensity perturbations.

After the identification of the structures in the narrow-band images in the wings of the spectral line, we considered several positions perpendicular to the structure, as shown in Fig. 1. At each position along the structure, we produce a time-distance

plot (TD, see for instance Fig. 2). The position of the structure, and its displacement in time can be estimated by locating at each temporal step, the minimum intensity (the structure appears as a dark S-shaped feature in time-distance diagrams). The position of the minimum $x(t)$ of the intensity at each time step (for each row in the time-distance plots) is estimated with sub-pixel accuracy (Mohamed et al. 2012) using a Fourier phase correlation method that relies on the estimation of the phase of the signal through Fast Fourier Transform (FFT). Since we deal with a complex Fourier function and work in Fourier space, we can estimate phase shifts of less than one pixel. Since we deal with a complex Fourier function and work in Fourier space, we can estimate phase shifts to less than one pixel. However, the actual shift resolution may be worse than this because of the limited length of some of the time-series and given the resolution dependency of the FFT on the length of the signal.

At the position of the minimum, the average value of the position of the structure $\langle x(t) \rangle$ is subtracted from $x(t)$ to separate the lateral fluctuations and the bulk motion. The lateral displacement of the structure $x(t)$ can be written as the sum of the lateral bulk motion $\langle x(t) \rangle$ and a perturbation term $\delta x(t)$:

$$x(t) = \langle x(t) \rangle + \delta x(t). \quad (1)$$

In this work, we mainly focus on the perturbation term that is related to the kink oscillations of the structure. The LOS motion was studied by analysing the evolution of the structure at several $H\alpha$ line positions. We used an image difference technique to track the LOS motion, where we subtracted the intensity images at the line-positions $H\alpha \pm 774 \text{ m\AA}$. Since these spicules are short lived and dynamic, such technique may lead to unrealistic signals and incorrect calculations of Doppler velocities. Hence, we also provide the structure's motion along the complete line scan as evidence of LOS motion.

We also studied compressive perturbations of the structure using the intensity variation $I(t)$ at the position of the minima in the TD diagrams. To increase the signal-to-noise ratio, we considered the average intensity within a region of three pixels, centred on the minimum. This was done for each time step (for each row in the TD diagrams, across all wavelength positions that show transverse motion), to obtain the variation of the intensity at each position along the structure. It is worth recalling here that the transverse movement of a flux tube due to kink-like perturbations is purely non-compressive, while the intensity enhancements reflect the changes in the radiative properties of the plasma by following the compression of the flux tube. For this reason, it is possible to consider the intensity perturbations as a consequence of compressive perturbations in the flux tube. However, we should keep in mind that many radiative effects (e.g. opacity effects or the variation of the height of formation of the spectral line) can also result in intensity changes, and particular care should be taken in interpreting the results. In the following subsections, we present two case studies.

3.1. Case 1 (Case 23 in Paper 1, Appendix A1)

The spicule is shown in the left panel of Fig. 1. It is observed in multiple wavelength positions with a small temporal offset in occurrence in the red wing and blue wing positions at $+516 \text{ m\AA}$ and -774 m\AA , respectively. There is some change in the LOS velocity component of this feature during its evolution. This event was first observed at 07:57:12 UT at $+516 \text{ m\AA}$ (corresponding to $t=0 \text{ s}$ in the TD diagrams). The evolution of the spicule at

$+516 \text{ m\AA}$ lasts for 120 s, with transverse oscillations in the image plane. The left panel in Fig. 1 shows the positions of eight slits (P1 – P8) plotted across the length of the spicule; between these eight positions we have obtained 21 TD diagrams. TD diagrams generated at two locations (P4 and P5) are presented in Fig. 2. We see the sinusoidal tracks that indicate a transverse oscillation at $+516 \text{ m\AA}$, but there is a fainter signal, at -774 m\AA . We plot observations related to line positions $+516 \text{ m\AA}$ and -774 m\AA in Fig. 3. Panels a and b show TD diagrams corresponding to P8 where tracks of the transverse motions are outlined with the solid white lines.

Panels c and d of Fig. 3 show the transverse displacements obtained from TD diagram for Case 1 represented in different colours and line styles. The displacement amplitude is $\sim 100 \pm 44 \text{ km}$ for the red wing, while a much larger variation is observed in the blue wing. Furthermore, from panels c and d of Fig. 3, we observe that the phase shift in the amplitude of the sinusoidal motion is not significant between the signals at different positions along the structure's length. Such behaviour may indicate that the observed oscillation is due to a standing MHD kink mode with a period of $\sim 45 \text{ s}$. In panels e and f of Fig. 3, we present normalised intensity and velocity from the TD diagrams at position P8. The transverse velocity amplitudes, estimated using derivatives of the transverse perturbations, are in the range of $\pm 7\text{--}10 \text{ km s}^{-1}$.

3.2. Case 2 (Case 8 in Paper 1, Appendix A1)

The right panel of Fig. 1 shows the second spicule analysed in this work. The solid white lines indicate the position of slits along the length of the spicule. Here we consider ten slit positions, viz. P1 – P10, and we have taken 31 slit positions between these two locations for the full analysis. This event (see Fig. 4) shows a LOS transverse motion of the flux tube. In Fig. 4 we show the evolution of this feature across six line positions along the $H\alpha$ line scan starting at 08:06:54 UT (corresponds to $t=0 \text{ s}$ in the TD diagrams) and ending at 08:07:34 UT. A yellow X marks the position of the spicule. This event is seen first in the red wing of $H\alpha$ line at $+516 \text{ m\AA}$ and $+774 \text{ m\AA}$. In the blue wing, we initially see a faint structure at 08:06:54 UT at the line position -774 m\AA .

The event then reappears in the red wing at $+516 \text{ m\AA}$. Figure 5 shows TD diagrams taken along the slits shown in the right panel of Fig.1. Sinusoidal (S-shape) tracks identified in $+516 \text{ m\AA}$ and $+774 \text{ m\AA}$ indicate transverse oscillations of the structure in the image plane. Therefore, this structure shows transverse oscillations along the LOS (along with the direction towards the observer) and in the image plane (along with the direction perpendicular to the observer), suggesting that the structure undergoes helical motions, which is a superposition of the two transverse oscillations.

Panels a and b of Figure 6 show the TD diagrams that are plotted for position P7 along the spicule with tracks of transverse motion over-plotted by solid white lines. Panels c and d of Figure 6 show the transverse displacements represented in different colours and line styles, obtained from TD diagrams for all 31 positions along the structure's length. There is no time delay within the measurement error between the oscillation signals confirming that there are no propagating disturbances along the length of the structure. Such a scenario indicates that the observed oscillation is due to a standing MHD kink mode. From the estimated displacement we find the maximum transverse velocity (v_k) to be $\pm 15 \text{ km s}^{-1}$. We note that the minima of the intensity coincide

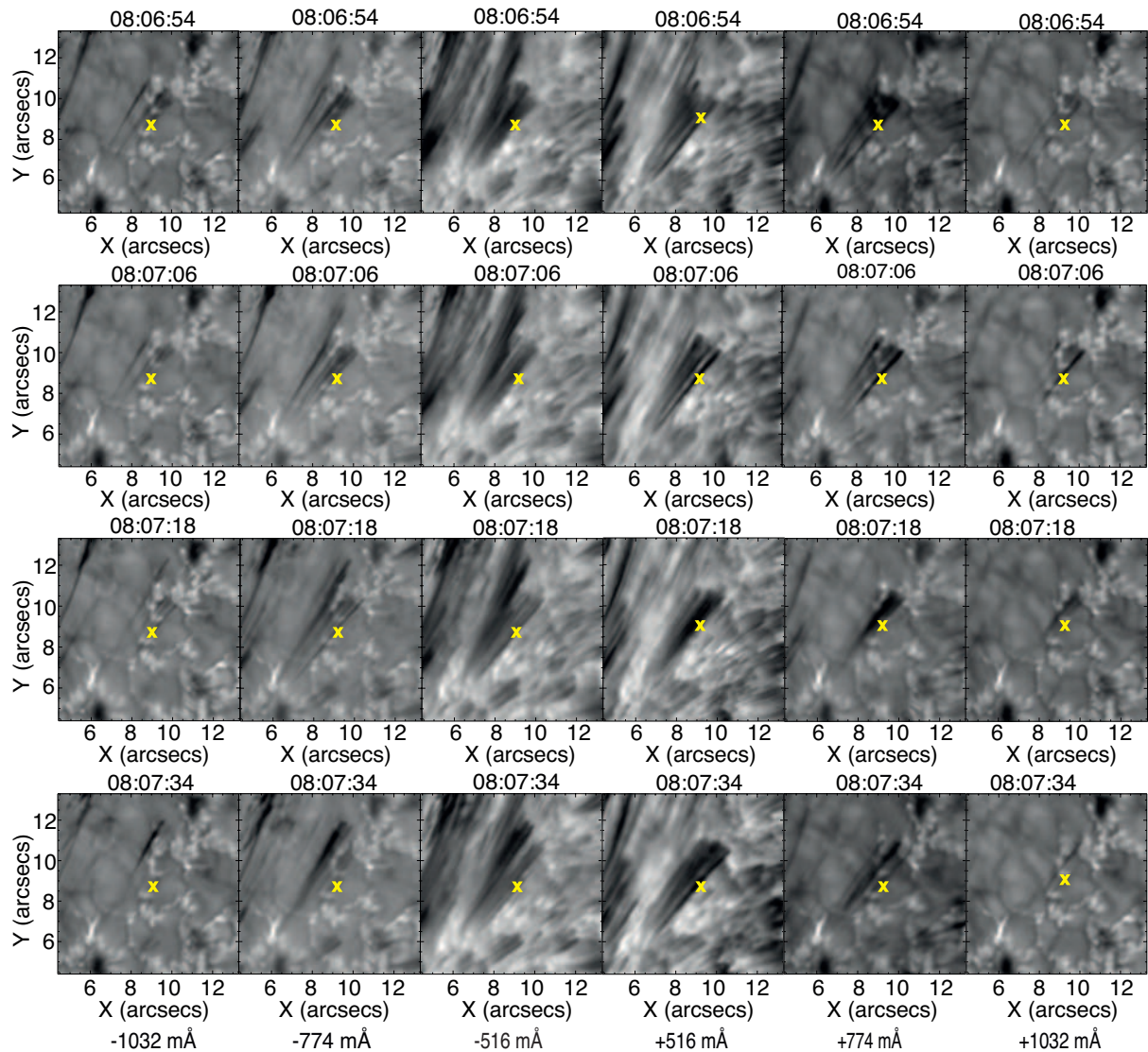


Fig. 4. Evolution of the second spicule (Case 2 in Fig 1) in $H\alpha$ as seen in six different ($\pm 516 \text{ mÅ}$, $\pm 774 \text{ mÅ}$ and $\pm 1032 \text{ mÅ}$ wavelength positions). An "X" indicates the position of the spicule. The event is first noted in the red-wing (at 08:06:54 UT, corresponding to $t=0$ s) in the TD diagrams and then in the blue wing.

with the reversal of direction of the structure's horizontal motion (see panels e and f of Figure 6).

3.3. Intensity and velocity relation for Cases 1 and 2

We have noted that the TD diagrams display minima of the intensity corresponding to the reversal of the direction of the motion of the flux tube. To better investigate this link, in the lower panels (e and f) of Figures 3 and 6, we plot the intensity perturbations and the horizontal velocity perturbations of the flux tubes obtained at two spectral positions. In both cases, we see that for every peak in intensity there are two peaks in velocity for the red wing, which may suggest a non-linear coherence between them. Moreover, in the blue wing, the intensity peaks correspond to velocity peaks, which indicates a linear correlation. For Case 1, the period between the two maxima is roughly 45 s (0.02 Hz frequency) whereas between two intensity minima it is 60 s (0.0116 Hz). For Case 2 the time-periods are 20 s (0.5 Hz) and 60 s (0.016 Hz) respectively.

4. Discussion and conclusions

We have presented two case studies of spicular-type events that display transverse oscillations (see Table A.1 for additional events). When the motion of the structures is polarised along the LOS, it is detected as a variation of the LOS (Doppler) velocity component that can result in the appearance or disappearance of the spicule, as observed in Paper1. When the motion is polarised in the image plane, we can identify the transverse motions in TD diagrams that are generated along the perpendicular cuts to the structure's axis. A combination of these two oscillations can result in a helical kink motion of the structure. Zaqarashvili & Skhirtladze (2008) studied the theoretical aspects of the helical motion in a magnetic flux tube. They showed that if two or more kink waves with different polarisations are excited in the same thin tube, then the superposition may set up helical motions of magnetic flux tubes in the photosphere/chromosphere. Here we detected simultaneous transverse motions in the image plane and along the LOS in the same structure (Figures 4 & 5), which can be interpreted as possible ev-

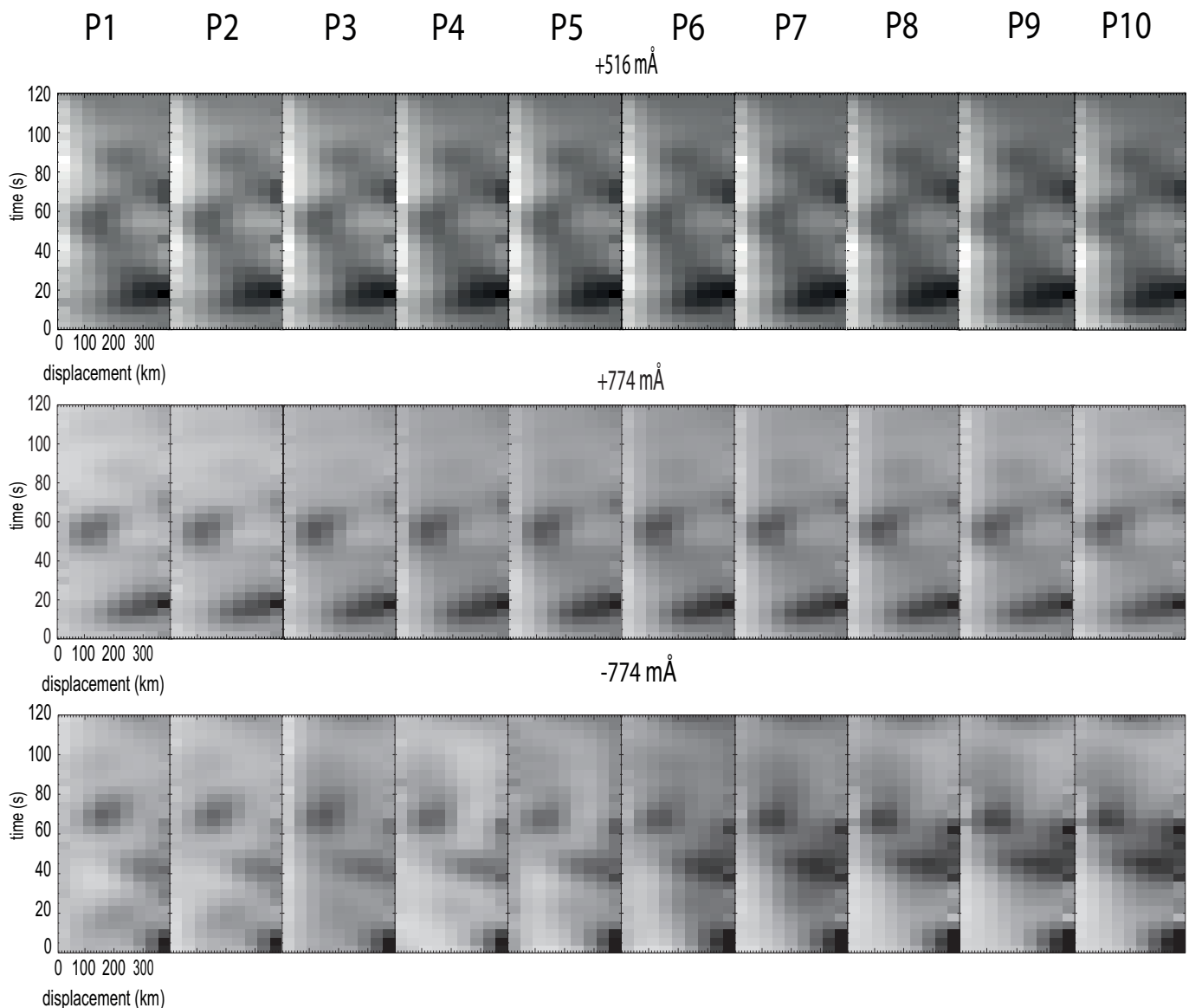


Fig. 5. Time-distance diagrams for the second spicule (Case 2) in 3 different positions of the $H\alpha$ line scan. TD diagrams are generated for 31 positions along the length of the structure (and between and including the 10 positions represented above), however, we have only presented 10 positions (P1 – P10) for clarity (see right panel of Fig. 1 to see positions of the 10 slits).

idence of helical kink motion in spicular-type events. We note that the observed transverse motions could arise as a result of a single kink wave that is polarised along the plane inclined from the LOS and the horizontal (image) instead of a 3D helical kink. If the observed wave is a helical kink wave then two orthogonal components of the transverse velocity are expected to oscillate in anti-phase. This means that the location of the maximum transverse velocity amplitude in the image plane should correspond to the location of the zero velocity along the LOS and vice versa. However, if a single kink wave causes the observed motion, then the two orthogonal components have to oscillate in phase. Unfortunately, our observations do not allow us to track the LOS velocity throughout the whole lifetime of the structure and investigate the phase relation between the two transverse components.

In panels e for Figure 3 and f for Figure 6, we show the relationship between intensity and velocity. We show that the min-

ima in intensity in the time-distance diagrams appear at the locations of inversion of the horizontal motion of the tube, suggesting coupling between compressive perturbations and transverse waves. Kink waves are non-compressive (their) restoring force is provided by magnetic tension), and are excited under the forcing action of the granular buffeting (see for instance Stangalini et al. 2014, and references therein). For this reason, kink waves are expected not to be associated with intensity enhancements, which is one of the manifestations of a change of the radiative properties of the local plasma due to compressive disturbances of a flux tube. However, our results show that there exists a link between the non-compressive kink oscillations, and the intensity perturbations that are observed in the flux tube. This is particularly evident in Figures 3 and 6, where corresponding to the inversion of the horizontal motion of the flux tube, one sees minima of the intensity perturbations.

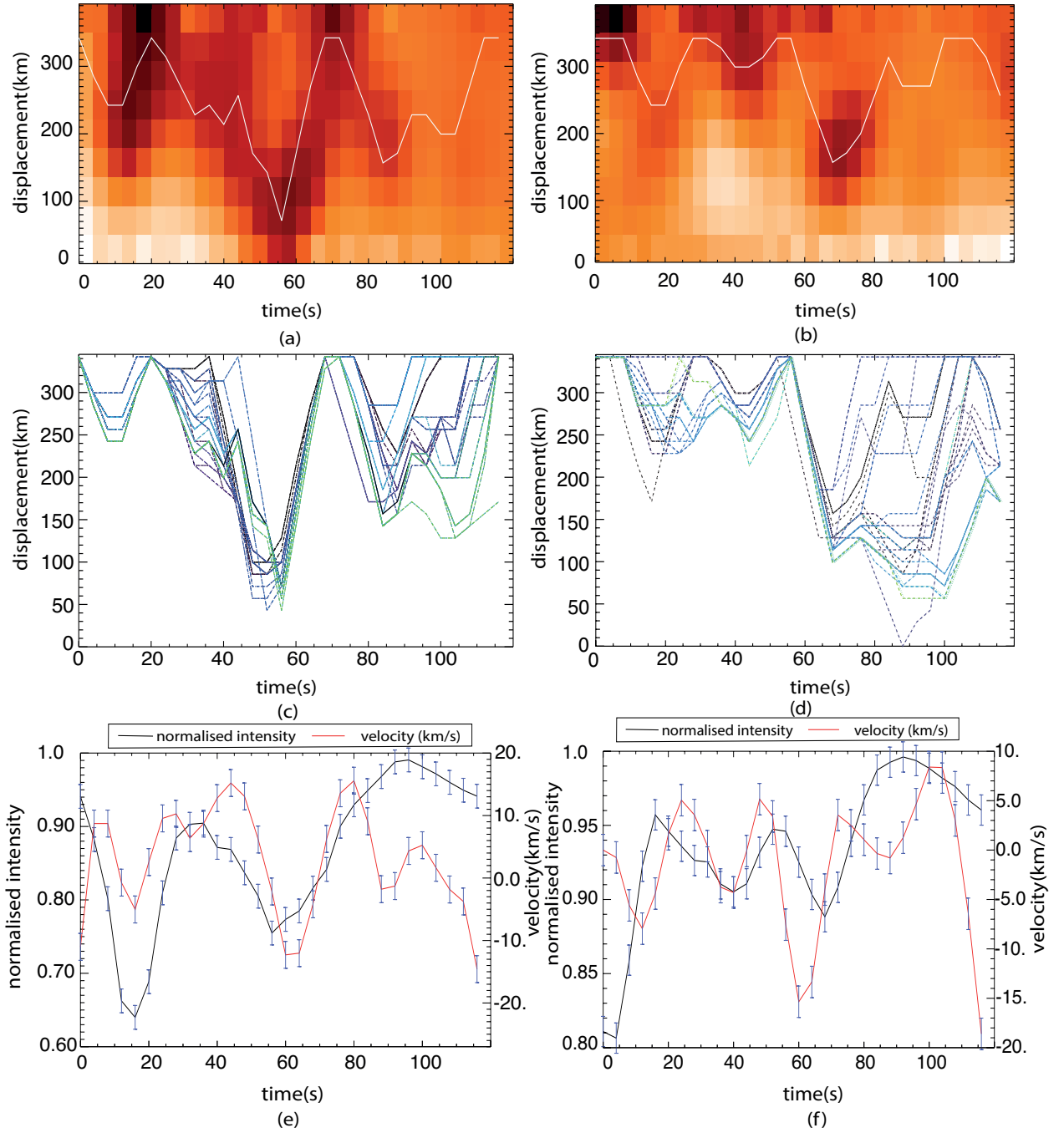


Fig. 6. Top panels (a and b): TD diagrams generated in wavelength positions $+774 \text{ mÅ}$ and -774 mÅ at location P8 for the second spicule (Case 2) with the minima corresponding to each time-step as outlined by the solid white line. The middle panels (c and d) show displacement time-series at 31 positions along the structure length (in between positions P1-P10). The bottom panels (e and f) show intensity vs time and velocity vs time behaviour. The red and the black solid lines are the velocity and intensity profiles, respectively. The error bars represent one standard deviation.

It must be noted that intensity perturbations may arise from several different radiative processes (e.g. opacity effects or thermal effects). However, in this case, there is evidence for a link with kink oscillations in the tube. In this regard, Stangalini et al. (2013) have shown, by exploiting high-resolution spectropolarimetric observations of small-scale flux tubes in the solar photosphere, that despite the non-compressive nature of kink waves, they can interact and possibly excite compressive waves. The authors noted that this scenario was consistent with Nakariakov & Verwichte (2005). Indeed, these authors have shown that compressive and non-compressive waves, cannot

only coexist in the same flux tube but that the kink mode can excite a longitudinal density perturbation, whose maximum is reached at the inversion points of the flux tube's horizontal motion. More recently, Stangalini et al. (2014) observed the excitation of kink sub-harmonics in small magnetic elements in the solar photosphere. They also noted that sub-harmonics can be considered as the signature of the chaotic excitation of kink waves in strongly non-linear systems. This condition of small flux tubes appears particularly favourable to the onset of nonlinear couplings between different modes as in Nakariakov & Verwichte (2005). In this regard, our findings

are in agreement with this scenario and suggest that coupling between compressive and non-compressive waves can also occur in the chromosphere. In this sense, our results represent the natural chromospheric extension of that already observed in small flux tubes in the photosphere.

Another possibility to explain the link between compressive perturbations and horizontal velocity is the interaction with the surrounding environment. From the temporal evolution, we see that these spicular-type events interact with other longer lived spicules. Such interactions may give rise to compression and intensity enhancements correlated to the horizontal displacement of the tube. This scenario is also in agreement with numerical simulations showing a weak coupling between kink and compressible fluctuations (see for example Jess et al. 2015).

5. Summary

Flux tubes serve as a medium to transport energy and mass across various levels of the solar atmosphere, through waves and plasma processes. Spicules and spicular-type events provide a medium to transfer these waves. In this article, we have reported observations of high-frequency waves in the solar chromosphere observed in spicular-type events. However, such waves are difficult to follow, and parameters such as density, temperature and energy are dependent on various factors. Therefore we need spectro-polarimetric data at high cadence. Such observations serve as inputs to theoretical models, which would further enable us to solve the puzzle of coronal heating.

The main findings from the paper are summarised as follows.

- In Case 1 we detected only image-plane motion, whereas in Case 2 we detected simultaneous transverse motions in the image plane and along LOS along the same structure.
- We presented possible evidence of helical kink motion in spicular-type events with a high-frequency source.
- We also find evidence for mode coupling between the compressive sausage modes (intensity variations) and the non-compressive kink mode (Figures 3 and 6). We speculate that such coupling could be driven by external factors such as the presence of other spicules and flows.

Acknowledgements. We thank the referee for their valuable comments. Armagh Observatory and Planetarium is grant-aided by the N. Ireland Department for Communities. The Swedish 1-m Solar Telescope is operated on the island of La Palma by the Institute for Solar Physics of Stockholm University in the Spanish Observatorio del Roque de los Muchachos of the Instituto í Astrofísica de Canarias. The authors wish to acknowledge the DJEI/DES/SFI/HEA Irish Centre for High-End Computing (ICHEC) for the provision of computing facilities and support. We also like to thank STFC, PATT and the Solarnet project which is supported by the European Commission's FP7 Capacities Programme under Grant Agreement number 312495 for T&S. JS is funded by the Leverhulme Trust. DK would like to acknowledge funding from the European Commission's Seventh Framework Programme (FP7/2007- 2013) under grant agreement No. 606862 (F-CHROMA). JS would like to thank INAF – Osservatorio Astronomico di Roma, 00040 Monte Porzio Catone (RM), Italy for assistance with the project. TR acknowledges the support from Science foundation of Ireland, grant number 11/REP.1/AST/3331. MS would acknowledge support from National Institute for Astrophysics through PRIN-INAF 2014

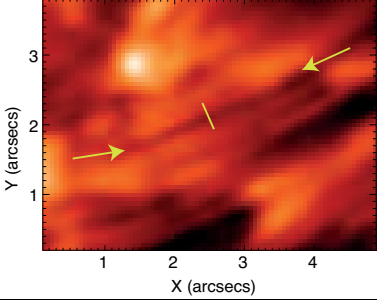
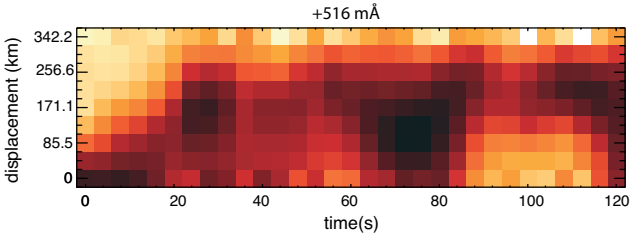
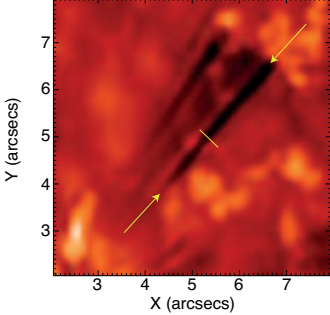
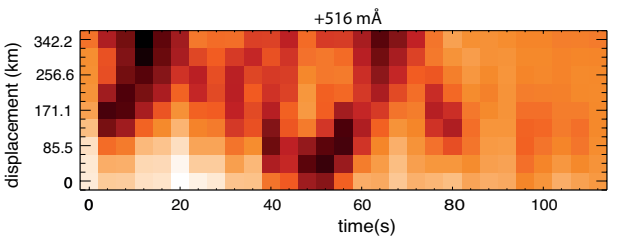
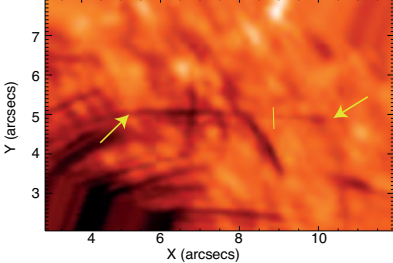
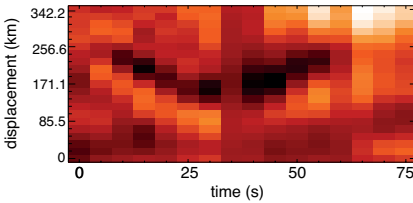
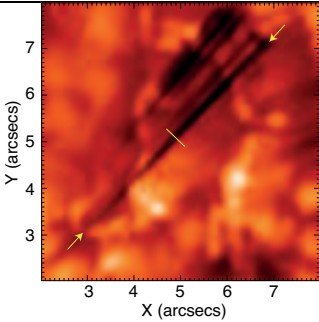
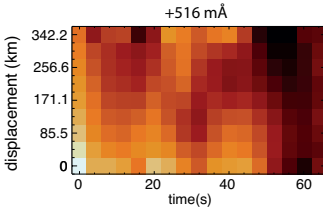
References

Beckers, J. M. 1968, *Sol. Phys.*, 3, 367
 Beckers, J. M. 1972, *ARA&A*, 10, 73
 Cranmer, S. R., van Ballegoijen, A. A., & Edgar, R. J. 2007, *ApJS*, 171, 520
 de la Cruz Rodríguez, J., Lofdahl, M. G., Sütterlin, P., Hillberg, T., & Rouppe van der Voort, L. 2015, *A&A*, 573, A40
 de la Cruz Rodríguez, J. & Socas-Navarro, H. 2011, *A&A*, 527, L8

De Pontieu, B., Carlsson, M., Rouppe van der Voort, L. H. M., et al. 2012, *ApJ*, 752, L12
 De Pontieu, B., Hansteen, V. H., Rouppe van der Voort, L., van Noort, M., & Carlsson, M. 2007a, *ApJ*, 655, 624
 De Pontieu, B., McIntosh, S., Hansteen, V. H., et al. 2007b, *PASJ*, 59, 655
 De Pontieu, B., McIntosh, S. W., Carlsson, M., et al. 2007c, *Science*, 318, 1574
 De Pontieu, B., Rouppe van der Voort, L., McIntosh, S. W., et al. 2014, *Science*, 346, D315
 He, J., Marsch, E., Tu, C., & Tian, H. 2009a, *ApJ*, 705, L217
 He, J.-S., Tu, C.-Y., Marsch, E., et al. 2009b, *A&A*, 497, 525
 Henriques, V. M. J., Kuridze, D., Mathioudakis, M., & Keenan, F. P. 2016, *ApJ*, 820, 124
 Jess, D. B., Morton, R. J., Verth, G., et al. 2015, *Space Sci. Rev.*, 190, 103
 Kikhianidze, V., Zaqarashvili, T. V., & Khutsishvili, E. 2006, *A&A*, 449, L35
 Kuridze, D., Henriques, V., Mathioudakis, M., et al. 2015, *ApJ*, 802, 26
 Kuridze, D., Morton, R. J., Erdélyi, R., et al. 2012, *ApJ*, 750, 51
 Kuridze, D., Verth, G., Mathioudakis, M., et al. 2013, *ApJ*, 779, 82
 Kuridze, D., Zaqarashvili, T. V., Henriques, V., et al. 2016, *ApJ*, 830, 133
 Langanen, Ø., De Pontieu, B., Carlsson, M., et al. 2008, *ApJ*, 679, L167
 Leenaarts, J., Carlsson, M., & Rouppe van der Voort, L. 2015, *ApJ*, 802, 136
 Mohamed, S. A., Helmi, A. K., Fkirin, M. A., & Badwai, S. M. 2012, *International Journal of Advanced Computer Science and Applications (IJACSA)*, 3, 4
 Morton, R. J., Verth, G., Jess, D. B., et al. 2012, *Nature Communications*, 3, 1315
 Nakariakov, V. M. & Verwichte, E. 2005, *Living Reviews in Solar Physics*, 2
 Nikolsky, G. M. & Platova, A. G. 1971, *Sol. Phys.*, 18, 403
 Okamoto, T. J. & De Pontieu, B. 2011, *ApJ*, 736, L24
 Pereira, T. M. D., De Pontieu, B., & Carlsson, M. 2012, *ApJ*, 759, 18
 Pereira, T. M. D., Rouppe van der Voort, L., & Carlsson, M. 2016, *ApJ*, 824, 65
 Rouppe van der Voort, L., Leenaarts, J., de Pontieu, B., Carlsson, M., & Vissers, G. 2009, *ApJ*, 705, 272
 Scharmer, G. B., Bjelksjö, K., Korhonen, T. K., Lindberg, B., & Pettersson, B. 2003, in *Society of Photo-Optical Instrumentation Engineers (SPIE) Conference Series*, Vol. 4853, *Innovative Telescopes and Instrumentation for Solar Astrophysics*, ed. S. L. Keil & S. V. Avakyan, 341–350
 Scharmer, G. B., Narayan, G., Hillberg, T., et al. 2008, *ApJ*, 689, L69
 Sekse, D. H., Rouppe van der Voort, L., & De Pontieu, B. 2013a, *ApJ*, 764, 164
 Sekse, D. H., Rouppe van der Voort, L., De Pontieu, B., & Scullion, E. 2013b, *ApJ*, 769, 44
 Shetye, J., Doyle, J. G., Scullion, E., Nelson, C. J., & Kuridze, D. 2016a, in *Astronomical Society of the Pacific Conference Series*, Vol. 504, *Coimbra Solar Physics Meeting: Ground-based Solar Observations in the Space Instrumentation Era*, ed. I. Dorotovic, C. E. Fischer, & M. Temmer, 115
 Shetye, J., Doyle, J. G., Scullion, E., et al. 2016b, *A&A*, 589, A3
 Stangalini, M., Consolini, G., Berrilli, F., De Michelis, P., & Tozzi, R. 2014, *A&A*, 569, A102
 Stangalini, M., Solanki, S. K., Cameron, R., & Martínez Pillet, V. 2013, *A&A*, 554, A115
 Tsiropoulou, G., Tziotziou, K., Kontogiannis, I., et al. 2012, *Space Sci. Rev.*, 169, 181
 van Noort, M., Rouppe van der Voort, L., & Lofdahl, M. G. 2005, *Sol. Phys.*, 228, 191
 Zaqarashvili, T. V. & Erdélyi, R. 2009, *Space Sci. Rev.*, 149, 355
 Zaqarashvili, T. V., Khutsishvili, E., Kikhianidze, V., & Ramishvili, G. 2007, *A&A*, 474, 627
 Zaqarashvili, T. V. & Skhirtladze, N. 2008, *ApJ*, 683, L91

Appendix A: Description of events

Table A.1. Examples of the wave signatures observed in Paper 1, where we show context images and time-distance diagrams corresponding to five events (four from the dataset of 10 June 2014 and one from 5 June 2014). The yellow arrows point towards the spicular-type events, and the solid yellow line indicates the location from, which the time-distance diagram is plotted. Here, we present the time-distance diagram taken at the central position along the feature’s length. Case 1 is a relatively isolated event that is best observed at $H\alpha$ +516 mÅ. Case 2 is a case of multiple close spicules that is observed in all positions in the $H\alpha$ wings. Case 3 only lasts half a cycle and is taken from 5 June 2014 as representative of events from that dataset with 5 s cadence. Cases 4 and 5 are similar to Case 2 discussed in this paper.

Case no	Context image	Time-distance diagrams
1 Case 23 in Paper 1, Appendix A1		
2 Case 8 in Paper 1, Appendix A.1.		
3 Case 1 in Paper 1, Appendix A.2		
4 Case 18 in Paper 1, Appendix A.1		
5 Case 12 in Paper 1, Appendix A.1	